

Investigation of Copper Removal from Aqueous Solution by Cement Kiln Dust as Industrial By-Product

Ahmed A. ElRefaey¹

ABSTRACT

This study investigated the copper (Cu^{+2}) removal from aqueous solution by cement kiln dust (CKD) as industrial by-product in cement manufacturing process. CKD was identified by Fourier transform infrared (FTIR), scanning electron microscopy (SEM) and surface areas show the differences of physicochemical properties. Batch equilibrium experiments were carried out at 20, 25 and 30 °C with time intervals extended to 96 h to investigate the efficiency of the CKD in the removal of Cu^{+2} . CKD expressed high affinity for removal of Cu^{+2} and was not affected by temperature or time. The removal of Cu^{+2} was indicated by changes of FTIR and SEM images before and after sorption experiments. The kinetic data were evaluated by fractional power, Elovich, pseudo-first order and pseudo-second-order kinetic models. The kinetic studies demonstrated that rate of the removal followed pseudo-second-order kinetic model ($r^2=0.99$). Thermodynamic parameters, the change of free energy (ΔG°), enthalpy (ΔH°) and entropy (ΔS°) were calculated for predicting the nature of adsorption. The parameters showed that the process was feasible, spontaneous and exothermic under experiment conditions. Solubility equilibrium for various expected copper compounds was estimated and the solubility of copper in Cu-CKD system suggested to be controlled by Cu CO_3 precipitation under experiment condition. The results indicated that CKD can be used as a low cost and effective sorbent for copper ions from aqueous solutions.

Key words: Copper, Cement Kiln Dust (CKD), Sorption Kinetics, Thermodynamic, Solubility Equilibrium

INTRODUCTION

Heavy metal pollution became critical serious environmental problems and public health issue. Heavy metals treatment is of special concern because of their recalcitrance, non degradable and persistence in the environment (Shareef, 2009 and Fenglian and Wang, 2011). Copper is a crucial micro-nutrients for most, if not all, living organisms and main component of numerous enzymes that are responsible for the oxidation–reduction reactions and has many commercial uses such as make electrical wiring, pipes, valves, coins, cooking utensils, building materials and in electroplating. Also, Copper is used through fertilizer, fungicides, algicides, insecticides, dyes manufacture and petroleum refining. Excess exposure and accumulation in living organisms can cause serious disturbances such

as headache, nausea, vomiting, diarrhea, cramps, convulsions, liver injury and acute poisoning to the human body or even death (Karabulut et al. 2000; Sobecka, 2001; WHO, 2004; Chen, 2005 and Paulino et al., 2006).

Generally, various technologies for elimination of heavy metal from wastewater have been used. These methods include chemical oxidation, reduction, chemical precipitation, solvent extraction, ion-exchange, adsorption, membrane filtration, coagulation-flocculation, flotation and electrochemical methods (Suzuki 1997; Ochie et al. 2008; Barakat, 2011; Fenglian and Wang, 2011). Among these methods, the adsorption can be an effective method in heavy metals treatment (Huang and Morehart, 1990; Bayat, 2002; Suzuki et al., 2005; Ahmad et al. 2010; Bilal et al. 2013). Huge economic sorbents can be used as materials which are abundant in nature or can be originated as a waste or byproduct from industry. Managing industrial by-product and wastes is a must to insure a clean and safe environment (Ibrahim et al., 2009).

Cement kiln dust (CKD) is a fine-grained solid material created as a by-product material in the kiln in the cement manufacturing process. Moreover CKD can be effectively used in removal heavy metals ions from solutions by adsorption as a low-cost and effective sorbent because of its high contents of alkali oxides, high surface area and excellent thermal resistance (Pigaga et al., 2005; Zaki et al. 2007; Rahman et al. 2011; Mackie and Walsh, 2012; Salem and Velayi, 2012; El-Refaey, 2016).

Therefore, the aim of this research is to investigate and evaluate the removal of copper (Cu^{+2}) from hazard aqueous solution by cement kiln dust as an industrial by-product. To achieve this aim, adsorption experiments were carried out at different temperatures with time interval extended to 96 h. Furthermore, the kinetic data were evaluated to fractional power, elovich, pseudo-first-order and pseudo second-order models to explain the reaction process and understand the sorption mechanism. Also, the thermodynamic parameters describing the nature of Cu^{2+} sorption onto CKD were examined. Finally, solubility equilibrium for various

¹Department of Soil & Water Science, Faculty of Desert and Environmental Agriculture, Alexandria University (Matrouh branch). Egypt; E-Mails: ahmedelrefaey@alexu.edu.eg
Received March 9, 2017, Accepted March 30, 2017

expected copper compounds were evaluated using solubility diagrams.

MATERIALS AND METHODS

Characterization of CKD

CKD was obtained from El-Amerya of cement plants, Alexandria, Egypt. Some Characteristics of CKD is record in table (1). The pH was measured in distilled water (1:2.5 H₂O). The major components of CKD are calcium carbonate of 47.6%; oxides of aluminum of 4.2%; iron of 2.8% and magnesium of 2.3%; free lime of 4.8% and some alkali salts such as sodium and potassium (Mahmoued, 2010, El-Refaey, 2016). Total carbon, nitrogen, hydrogen content and sulfur in CKD were determined by CHNS analyzer (Elementar, Vario EL, Germany) (Table.1).

The specific surface area of CKD was determined from N₂ adsorption isotherms at 77 K using a gas sorption analyzer (Beckman Coulter SA(TM) 3100 Surface Area and Pore Size Analyzer). Brunauer–Emmett–Teller (BET) adsorption isotherms equation was applied to calculate surface areas. The pore size distribution was determined by the Barrett–Joyner–Halenda (BJH) method from the N₂ desorption isotherms (Park and Komarneni, 1998; Nader, 2015).

The Fourier transform-infrared (FTIR) spectra were obtained at the range 400 – 4,000 cm⁻¹ by a Fourier transforms infrared spectrometer (model FT/IR-5300, JASCO Corporation, Japan) using KBr pellet method. A small sample of powder charcoal was amounted on a potassium bromide (KBr) disc which had been earlier scanned as a background in the FTIR analysis. FTIR were measured before and after sorption experiments.

Scanning electron microscopy (SEM) was performed by using a Phillips SEM-505 scanning electron microscope and operated at 300 kV/SE and 50 °C inclination. Before examination, samples were coated with gold in a sputter-coating unit (Edwards Vacuum Components Ltd, Sussex, UK) for electrical conduction. CKD samples were dried overnight at approximately 105 °C under vacuum before SEM examination. SEM images were obtained at various magnification scales before and after sorption experiments.

Sorption experiments and analytical methods

Separate suspensions (4 g /0.8L in 0.01 M KCl) were shaking end-over-end at 300 rpm for 24 h to reach equilibrium. At the initial time, pH measured then adding Cu (II) to each reactor as Cu Cl₂, for the final

concentration of 1.5 mM in each reactor. The adsorption isotherm was conducted at 20, 25 and 30°C for intervals extended to 96h. Suspensions were filtered (0.45 µm) immediately following the pH measurement. Metal ion concentrations were measured in Filtrate using Atomic Absorption Spectrophotometer Varian Spectra (model 220). All measurements, Metal concentrations and pH measurements were determined in duplicate.

The adsorption amount (q_t) and the percentage of adsorption (S %) is calculated according to:

$$q_t = \frac{(c_0 - c_t)V}{m} \quad (1)$$

$$S\% = \frac{(c_0 - c_t)}{c_0} \quad (2)$$

Where q_t is the metal ion adsorption amount at time t (mg/g), S% is the adsorption percentage (%), m is the weight of CKD sample (g), V is the solution volume (dm³), and c₀ and c_t are the initial and equilibrium concentrations of Cu⁺⁺ ions in solution, respectively.

Solubility equilibrium estimation

Solubility measurements in Cu treated CKD aimed at predicting indirectly the solid phases controlling the copper concentration through calculating their ion activity products. Compounds of these solid phases to ionize and form complexes in solution. Davies equation was employed for estimating the single ion activity coefficient (γ_i) in solution for the ionic species (i).

$$\log \gamma_i = -A Z_i^2 [(\sqrt{I} / \sqrt{1+I}) - 0.3I] \quad (3)$$

where A is equals 0.509 for water at 25°C and is a temperature dependant constant (Lindsay (1979), Z_i is the valence of the solute and I is the ionic strength (< 0.5 mol/L) of the solution based on concentration expressed in mol/L and can calculated from the flowing equation (Griffin and Jurinak, 1973):

$$I = 0.013 \text{ EC} \quad r^2 = 0.99 \quad (4)$$

Where EC is electrical conductivity expressed on dS/m at 25°C. With r² of 0.99 indicates a very high correlation between calculated ionic strength (I) by the above empirical equation that based on Debye–Hückel equation ($I = \frac{1}{2} \sum C_i Z_i^2$) where C_i is the concentration in mol/L of ion (i). This empirical relationship is particularly useful when the complete composition of an aqueous solution is unknown or where ion pair formation in solution. The ions activities of interested cations (Cu²⁺, Ca²⁺ and H⁺) and anions (Cl⁻, HCO₃⁻, CO₃⁼ and OH⁻) were estimated.

Table 1. Some Characteristics of CKD

pH	C %	H %	N %	S %	Total CaCO ₃ %	Surface area m ² g ⁻¹	Total pore volume mm ³ g ⁻¹
10.20	6.35	0.19	Nil	0.84	47.60	20.98	37.30

RESULTS AND DISCUSSION

Characteristics of CKD

Surface area and pore analysis

The BET technique was used to determine the specific surface area of CKD samples. The adsorbed N_2 per gram of sample was plotted versus the relative vapor pressure (P/P_0) of N_2 and exhibiting a smoothed lap rising up at high relative pressures with changing degrees of slope (Fig. 1). The data were evaluated by the Brunauer–Emmett–Teller (BET) equation to calculate surface area. The apparent specific surface area of CKD was $20.98 \text{ m}^2/\text{g}$ and total pore volume for CKD was $37.30 \text{ mm}^3/\text{g}$ (Table 1). Desorption BJH pore size distribution for CKD was identified in Table 2. The pore diameter of $<6 \text{ nm}$ is the highest percent range between all pore diameter ranges. Therefore, the BJH pore diameters and pore volumes in CKD tends to relate to micropores. Micropores contribute to principally surface area, while macropores contribute as a channel to micropore surfaces (Yahya *et al.*, 2015).

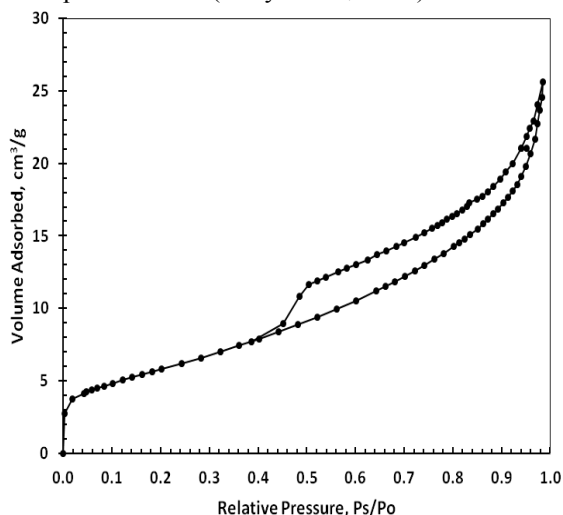


Fig 1. N_2 -adsorption isotherms of CKD

FTIR analysis

FTIR techniques were conducted to identify the functional groups of CKD before and after the sorption of Cu ions from aqueous solutions (Figure 2). The FTIR spectrum of CKD shows peak positions at $3,433.06$, $1,454.23$, and $1,095.49 \text{ cm}^{-1}$. The band at $3,433.06$ is appropriate to O–H (hydroxyl) while the bands at $1,454.23$ and $1,095.49$ reflect the carbonate and silicate; similar data were obtained by (Al-Ghouti *et al.*, 2003; Saraya and Aboul-Fetouh 2012; El-Refaey, 2016). Most studies utilize FTIR just to verify the availability of certain surface functional groups as part of sorbents structure, although probing the influence of these groups

in relation to the metal binding process is also possible (Ochie *et al.* 2008). The comparison of CKD before and after the sorption of Cu ions showed slight shifts in FTIR bands with reducing transmission percentage at carbonate band (from 5.253 to 1.745%) after sorption reaction (Figure 2). This confirms the attachment of copper ions on CKD surfaces.

Table 2. Desorption Barrett-Joyner-Halenda (BJH) pore size distribution of CKD

Pore diameter range nm	Pore volume	
	ml/ g	%
> 80	0.00283	7.88
20 - 80	0.00955	26.55
16 - 20	0.00217	6.02
12 - 16	0.00182	5.07
10 - 12	0.00170	4.74
8 - 10	0.00158	4.40
6 - 8	0.00276	7.68
< 6	0.01355	37.67

Scanning electron microscopy (SEM)

The surface structure of CKD was analyzed by SEM before and after Cu^{+2} sorption experiments. The textural and morphological structure examination of CKD can be observed from the SEM photographs at $\times 5,000$ and $\times 10,000$ magnification (Figure 3). It was observed that CKD have the finest particle sizes and the sharp changes that were observed in porous structure of CKD. The CKD particles were covered by precipitates or complexes formation after sorption experiments. This may indicate various mechanisms for Cu^{+2} removals.

Copper removal

CKD showed a strong affinity to remove most Cu^{+2} after 10 min of the reaction, where $> 90\%$ of the removal at first 10 min increased to more than 99% after 1 h (Fig. 4). The effect of temperature on Cu^{+2} removal by CKD was not significant. The effect of temperature on Cu^{+2} removal reactions was not observed with CKD. El-Refaey (2016) found the same trend of Cd^{+2} removals by CKD. Removal of Copper by CKD was time and temperature independence that might reflect the retention mechanisms. The pH has significant role in heavy metals removal. As presumed, the proceeding of Cu^{+2} removals by CKD favored with pH increases. The pH increased gradually from 6.70, 6.40 and 6.40 to 8.2, 8.39 and 8.4 at 20°C , 25°C and 30°C , respectively after 96 h. According to proposed mechanisms of metal ion binding to active surface of materials, Cu^{+2} removal could be achieved by electrostatic interaction with negatively charged surface functional groups (cation exchange), specific metal–ligand complexation involving surface functional groups of sorbents and/or physical sorption controlled by surface area and porosity

(Brown, *et al.*, 2000; Uchimiya *et al.*, 2010; Saleh *et al.* 2016). Evidence from the present results confirmed that intervention of more than one mechanism can be proposed to control the removal process of Cu^{+2} depending on the sorbent characteristics, supported by the sharp changes in SEM images before and after sorption experiments of CKD (fig 3). The high efficacy

of Cu^{+2} removal process by CKD could be explained by increasing pH solutions, calcium carbonate and calcium oxide contents, surface area, oxide content, and reducing metal solubility owed to enhanced sorption and/or precipitation (Zaki *et al.*, 2007; Hal *et al.*, 2012; Mackie and Walsh, 2012; El Zayat *et al.*, 2014).

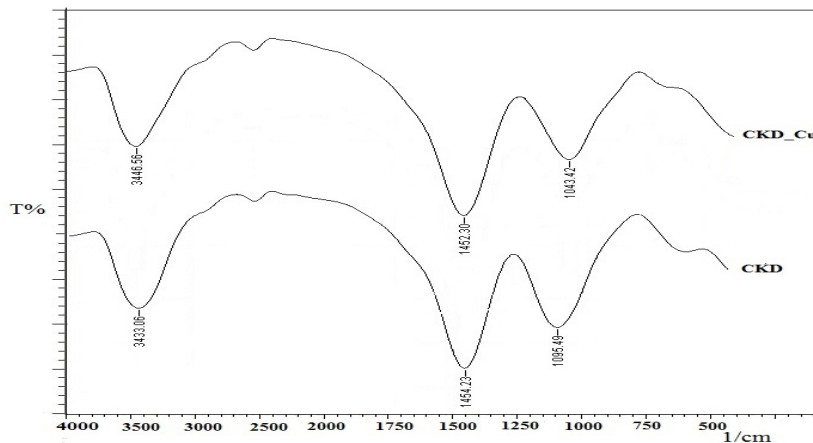


Fig 2. FTIR spectra of the CKD before and after the sorption of Cu ions experiments

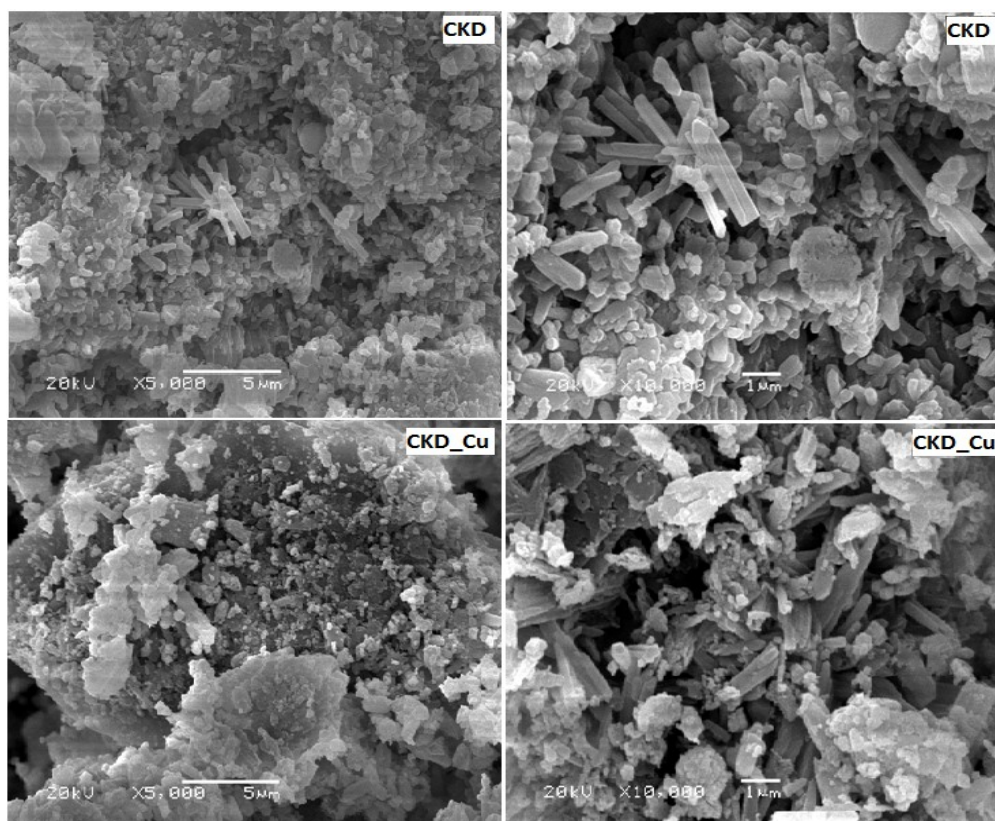


Fig 3. Scanning electron micrographs (SEM) of CKD before and after the removal reactions of Cu ions from aqueous solutions at 25 °C

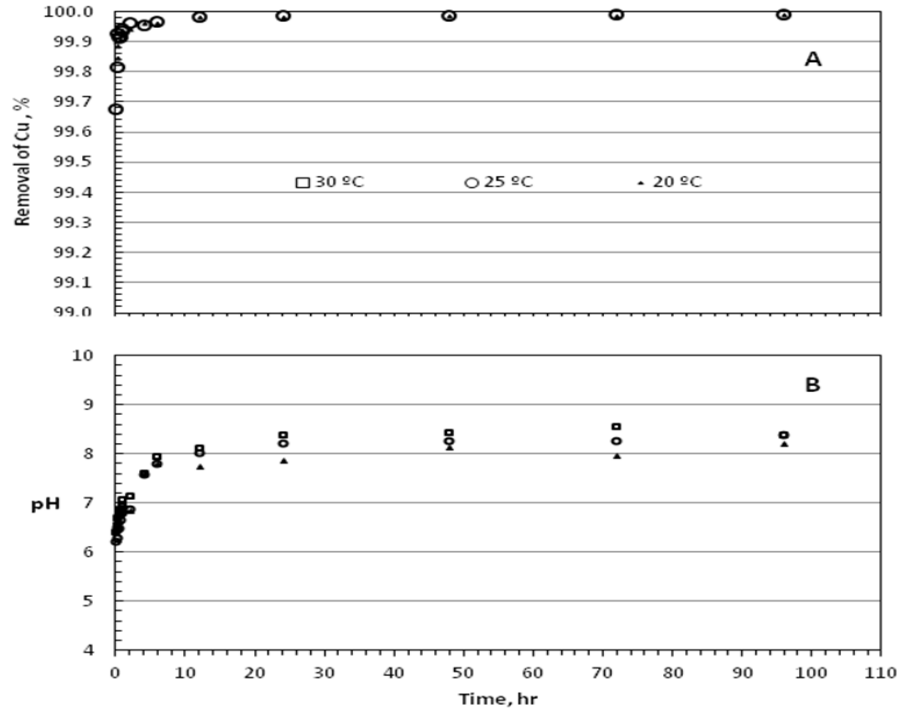


Fig 4. Removal of copper ions (A) and pH of aqueous solution (B) by CKD as a function of time and temperature

Kinetic studies

The fractional power, elovich, pseudo-first-order and pseudo-second-order kinetics models were applied. The fractional power model is an amended of the Freundlich equation and can be expressed by Equation (5) (Ho and McKay, 2002) or its linear form as given in equation (6):

$$q_t = a t^b \quad (5)$$

$$\ln q_t = \ln a + b \ln t \quad (6)$$

where q_t is the amount of Cu^{+2} sorbed by CKD at a time t , while a and b are constants with $b < 1$; ab is the specific sorption rate at unit time.

Elovich equation is useful model that can describe in a semi-empirical equation (Inyang et al., 2016), which is given by equations (7 and 8):

$$\frac{dq_t}{dt} = \alpha \exp(-\beta q_t) \quad (7)$$

or in integrated form:

$$q_t = \frac{1}{\beta} \ln \alpha \beta + \frac{1}{\beta} \ln t \quad (8)$$

where α is the initial rate of adsorption (mg/g. min), and β is related to the surface coverage extent and activation energy for chemisorption (g/mg). Thus, the

slope and intercept of the linear plot of q_t versus $\ln t$ give the constants.

The pseudo-first-order model (Lagergren, 1898) was applied and is given by:

$$\text{Log}(q_e - q_t) = \text{Log } q_e - k_1 t / 2.203 \quad (9)$$

where k_1 is the pseudo-first-order rate constant (min^{-1}) and q_e (mg g^{-1}) is the adsorption capacity at equilibrium and q_t (mg g^{-1}) is the amount of metal adsorbed at any time(t). Also, pseudo-second-order model (Ho, 2006) was applied and is expressed as:

$$\frac{t}{q_t} = \frac{1}{k_2 q_e^2} + \frac{t}{q_e} \quad (10)$$

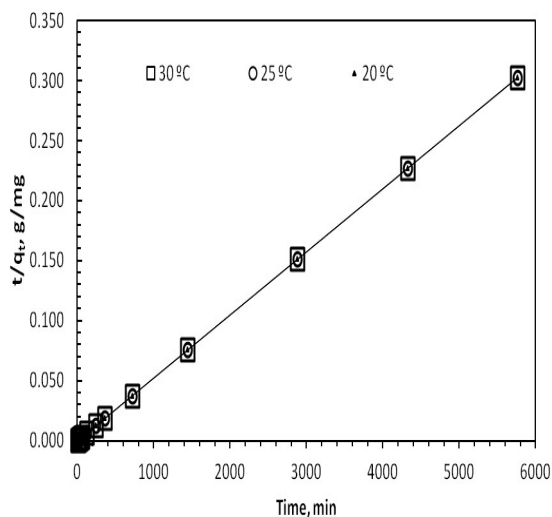
where k_2 ($\text{g mg} / \text{min}$) is the pseudo-second-order rate constant. The values of q_e , k_1 and k_2 were obtained from the slopes and intercepts of the adsorption Fractional power, kinetic models have been applied to estimate the rate-controlling mechanism of the adsorption process. The parameters are recorded in Table 3, where a and b are constants related to specific sorption rate, α is the rate of initial adsorption ($\text{mg} / \text{g. min}$), β is the desorption constant ($\text{g mg} / \text{min}$), q_e can be regarded as the amounts of metals adsorbed on the adsorbent (mg / g) at equilibrium, k_1 and k_2 and min^{-1} is the rate constant, respectively.

Table 3. Kinetic parameters of Cu⁺² on CKD at various temperatures

Model	20°C	25°C	30°C
Fractional power			
A	3809.54	3808.02	3809.54
B	1.60×10^{-4}	2.90×10^{-4}	1.80×10^{-4}
r ²	0.91	0.59	0.85
Elovich			
A	2.38×10^{71}	3.00×10^{58}	7.63×10^{67}
B	1.69	0.91	1.48
r ²	0.91	0.60	0.85
Pseudo-first-order			
q _e	15244.35	15244.35	15244.35
K ₁	2.00×10^{-6}	3.00×10^{-6}	2.30×10^{-6}
r ²	0.43	0.19	0.42
Pseudo-second-order			
q _e	3812.43	3812.43	3812.43
K ₂	0.34	0.38	0.34
r ²	0.99	0.99	0.99

From the kinetic parameters which have been calculated at different temperatures and times listed in Table 3, the high values of the coefficient of determination ($r^2 > 0.99$) confirmed that the pseudo-second-order model was most adequate to represent the adsorption kinetics of Copper onto CKD.

Moreover, experimental q_e values are very close to those predicted from the pseudo-second-order kinetic model ($r^2 > 0.99$). Therefore, the obtained results indicated that the adsorption of Cu⁺² could be best described by the pseudo-second-order model (Fig. 5).

**Fig 5. Pseudo-second-order plots for Cu⁺² removal kinetics by CKD at different temperatures**

Thermodynamic studies

Thermodynamic considerations of the sorption process are essential to identify whether the process is spontaneous or not and understanding the removal mechanisms. Thermodynamic parameters such as Gibbs free energy change (ΔG°), enthalpy change (ΔH°) and the entropy change (ΔS°) can be estimated using equilibrium constants changing with temperature. Spontaneity of a chemical reaction can be indicated by the changes in the Gibbs free energy and therefore is an important criterion for spontaneity (Ucun et al., 2008). The thermodynamic parameters (ΔH° , ΔG° and ΔS°) were calculated from the sorption data. The Gibbs free energy change of the reaction was calculated from equation (11) (Kılıç et al., 2013):

$$\Delta G^\circ = -RT \ln K_L \quad (11)$$

where R is gas constant (8.314 J/mol K), K_L is equilibrium constant and T is absolute temperature (K). The K_L value was determined using equation (12):

$$K_L = \frac{q_e}{C_e} \quad (12)$$

where q_e and C_e is the equilibrium concentration of metal ions on adsorbent (mg/g) and in the solution (mg/L), respectively. Relations between ΔG° , ΔH° and ΔS° can be expressed by the following equations:

$$\Delta G^\circ = \Delta H^\circ - T \Delta S^\circ \quad (13)$$

Eq (11) can be rewritten as

$$\ln K_L = -\frac{\Delta G^\circ}{RT} = -\frac{\Delta H^\circ}{RT} + \frac{\Delta S^\circ}{R} \quad (14)$$

According to Eq. (14), ΔH° and ΔS° parameters can be obtained from the slope and intercept of the plot of $\ln K_L$ versus $1/T$, respectively (Meena et al., 2008; Sari et

al., 2007; Uzun et al., 2008, Kılıc *et al.*, 2013). The calculated values of Gibbs free energy change (ΔG°), enthalpy (ΔH°), and entropy (ΔS°) are given in Table (4). The negative values of ΔG° indicate that the process is thermodynamically feasible and spontaneous. The negative value of ΔH° pointed out that the nature of adsorption process is exothermic. The positive value of ΔS° reflects the affinity of CKD for Cu^{2+} and suggests increasing in randomness at the solid/solution interface during the removal process.

Table 4. Thermodynamic parameters of the removal of Cu^{2+} by CKD from aqueous solutions

T°C	ΔG° kJ/mol	ΔS° J/mol K	ΔH° kJ/mol
20	-18.17		
25	-18.58	2.14	- 0.37
30	-19.66		

Copper solubility behavior

The sorption isotherm results for CKD (47% CaCO_3) showed a higher affinity of surfaces to Cu ions. The pH and carbonate contents are known to play a major role in influencing the solubility as well as sorption processes in experiments condition. A decrease in soluble Cu^{2+} was accompanied with the increase of pH values (Fig. 6). Ion activity of copper was computed during Cu reaction with CKD for interval time of 10 min, 1, 2, 6

and 24 h. In an attempt to figure out the probability of Cu compounds formation under the experiment conditions, copper activities was calculated for drawing the solubility isotherms lines of CuCO_3 , Cu(OH)_2 , $\text{Cu}_2(\text{OH})_2\text{CO}_3$, $\text{CuSO}_4 \cdot 5\text{H}_2\text{O}$, $\text{Cu}_4(\text{OH})_6\text{SO}_4$ and CaCO_3 at atmospheric partial pressure of carbon dioxide ($\text{PCO}_2 = 10^{-3.52}$ atm) on the solubility diagram of Log Me^{2+} -pH using solubility constants given by Lindsay (1979). The computed ion activities of Cu^{2+} and Ca^{2+} for CKD suspensions were plotted on Log Me^{2+} -pH diagram (Fig. 6). The computed copper activities for CuCO_3 were found to be lower than the solubility products of their minerals during the reaction time. (Fig. 6-A). Opposing to that, the computed copper activities were higher than calculated solubility that based on the actual experimental partial pressure of CO_2 (Fig. 6-B). The apparent discrepancy is due to the differences in P CO_2 as a basis for the calculation, as P CO_2 was not constant during the experimental time. The partial pressure of CO_2 in Cu-CKD (47% CaCO_3) suspensions was estimated using pH value and solution HCO_3^- activity and it was ranged from 0.021 to 0.0018 atm. The calculated copper activities values for CKD (47%) showed porobability of Cu^{2+} precipitation after six hours (Fig. 6-B). On other hand, results pointed out that Cu precipitation had no effect on CaCO_3 solubility of CKD (Fig. 6-A and B).

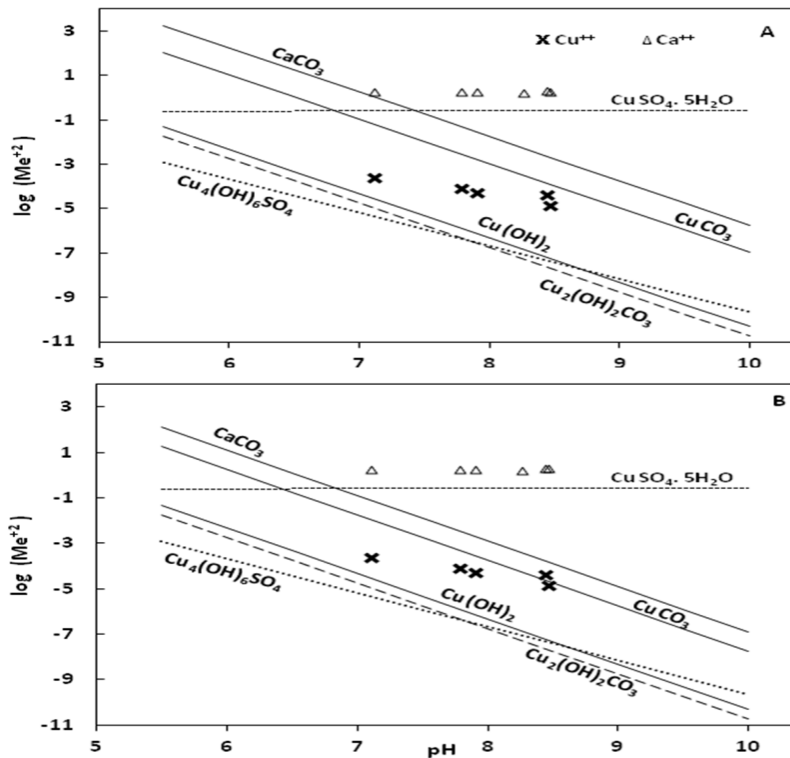


Fig. 6. Calculated ion activities of Cu^{2+} and Ca^{2+} for CKD suspensions (A) $\text{Log PCO}_2 = -3.52$ atm and (B) $\text{Log PCO}_2 = -2.36$ atm (actual experimental condition)

The calculated CaCO_3 solubility product indicates very high super saturation; CaCO_3 may be highly dissolved due to high chloride concentration as background solution. Conducting solubility experiments with controlled PCO_2 is needed to differentiate between possibilities of forming CuCO_3 , Cu(OH)_2 or $\text{Cu}_2(\text{OH})_2\text{CO}_3$, $\text{CuSO}_4 \cdot 5\text{H}_2\text{O}$ and $\text{Cu}_4(\text{OH})_6\text{SO}_4$ compounds and find out their effect on $\text{CaCO}_3/\text{CaSO}_4$ solubility (Lindsay 1979; Sposito, 1989).

Ion activity product, IAP can also be used as a guide in determining the achievement of dissolution equilibrium. This can be obtained by examining measured value of relative saturation (Ω) for different solid phase (Sposito, 1989):

$$\Omega = \text{IAP} / K_{\text{so}} \quad (15)$$

Where K_{so} is the solubility product constant and IAP is the ion activity product. If Ω is less than 1, the solution will be under saturated. Otherwise, if Ω is more than 1, the solution will be super saturated and when the solution reaction is at equilibrium Ω is equals 1. Figure (7) shows the approach of Ω with respect to CuCO_3 , Cu(OH)_2 and $\text{Cu}_2(\text{OH})_2\text{CO}_3$ compounds during reaction time. For Cu(OH)_2 and $\text{Cu}_2(\text{OH})_2\text{CO}_3$, Ω is super saturated all over the study time. On other hand Ω for CuCO_3 tends to move from under saturation during the first two hours of reaction to reach equilibrium and be super saturation after 6 hours. Therefore, the solubility of Cu^{++} in Cu-CKD system under experiment condition may be controlled by CuCO_3 precipitation. This assumption is confirmed not only by shifting of FTIR band but also by reducing transitions percentage (5.253 to 1.745) of FTIR carbonate band (1454.23 cm^{-1}) after copper reaction with CKD.

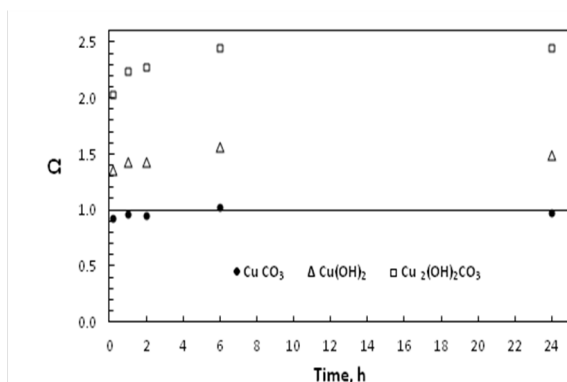


Fig. 7. Estimated value of relative saturation (Ω) for CuCO_3 , Cu(OH)_2 and $\text{Cu}_2(\text{OH})_2\text{CO}_3$ compounds in Cu-CKD suspensions during reaction time

CONCLUSION

The results pointed out that the potential of CKD for removing Cu^{2+} from aqueous solutions within the first 10 min of the batch reaction preceded with no effect by temperature or time. The high efficacy of CKD explained by increasing pH solutions, high content of calcium carbonate, surface area, oxide content, and reducing metal solubility owed to enhanced sorption and/or precipitation. The pseudo-second-order kinetic model agrees very well with the dynamic behavior for the removal of Cu^{2+} . The negative values of ΔG° indicated spontaneity and feasibility of the adsorption process. The negative value of ΔH° shows that the nature of adsorption process is exothermic. The positive value of ΔS° explains the affinity of Cu^{++} for CKD during the removal process. The solubility study of Cu-CKD system suggested that CuCO_3 precipitation could control copper solubility under experimental condition. That was confirmed by shifting and reducing transmission percentage of FTIR carbonate band.

ACKNOWLEDGE

The author thanks Prof. Maher Saleh for his support, helpful cooperation, and offering lab facilities.

REFERENCES

- Ahmad, R., R. Kumar and S. Haseeb. 2010. Adsorption of Cu^{2+} from aqueous solution onto iron oxide coated eggshell powder: Evaluation of equilibrium, isotherms, kinetics, and regeneration capacity. *Arabian Journal of Chemistry* 5: 353–359.
- Al-Ghouti, M. A., M. A. M. Khraisheh, S. J. Allen and M. N. Ahmad. 2003. The removal of dyes from textile wastewater: a study of the physical characteristics and adsorption mechanisms of diatomaceous earth. *Journal of Environmental Management* 69: 229–238.
- Barakat, M.A. 2011. New trends in removing heavy metals from industrial wastewater. *Arabian Journal of Chemistry* 4:361–377.
- Bayat, B. 2002. Comparative study of adsorption properties of Turkish fly ashes. II. The case of chromium (VI) and cadmium (II). *Journal of Hazardous Materials*, B95 : 275–290.
- Bilal M., J.A. Shah, T. Ashfaq, S.M.H. Gardazi, A.A. Tahir, A. Pervez, H. Haroon and Q. Mahmood 2013. Waste biomass adsorbents for copper removal from industrial wastewater – A review. *Journal of Hazardous Materials* 263: 322–333.
- Brown, P.A., S.A. Gill and S.J. Allen. 2000. Metal removal from wastewater using peat. *Water Res.* 16: 3907–3916.
- Chen, X. C., Y. P. Wang, Q. Lin, J. Y. Shi, W. X. Wu and Y. X. Chen. 2005. Biosorption of copper(II) and zinc(II) from aqueous solution by *Pseudomonas putida* CZ1. *Colloids and Surfaces B: Biointerfaces* 46: 101–107.

- El Zayat, M., S. Elagroudy and S. El Haggag. 2014. Equilibrium analysis for heavy metal cation removal using cement kiln dust. *Water Science & Technology* 70: 1011–1018.
- El-Refaey, Ahmed A. 2016. Comparative performance of cement kiln dust and activated carbon in removal of cadmium from aqueous solutions. *Water Science & Technology* 73: 1691–1699.
- Fenglian Fu and Q Wang. 2011. Removal of heavy metal ions from wastewaters: A review. *Journal of Environmental Management* 92: 407–418.
- Griffin, R. A. and J.J. Jurinak. 1973. Estimation of activity coefficients from the electrical conductivity of natural aquatic systems and soils extracts. *Soil Sci.* 116:26–30.
- Hal, B., L.Evans and R. Lamber. 2012. Effects of cement or lime on Cd, Co, Cu, Ni, Pb, Sb and Zn mobility in field-contaminated and aged soils. *Journal of Hazardous Materials* 199–200: 119–127.
- Ho, Y. S. 2006. Second-order kinetic model for the sorption of cadmium onto tree fern: a comparison of linear and nonlinear methods. *Water Research* 40: 119–125.
- Ho, Y. S. and G. McKay. 2002. Application of kinetic models to the sorption of copper (II) on to peat. *Adsorption Science & Technology* 20: 797–815.
- Huang, C.P., and A.L. Morehart. 1990. The removal of Cu (II) from dilute aqueous solutions by *Saccharomyces cerevisiae*. *Water Research* 24: 433–439.
- Ibrahim, H.G., A.Y. Okasha and M. S. ElAtrash. 2009. Using cement kiln dust to treat tannery wastewater effluents. 11th international conference on Environmental science and Technology Crete, Greece.
- Inyang, H. I., A. Onwawoma, and S. Bae. 2016. The Elovich equation as a predictor of lead and cadmium sorption rates on contaminant barrier minerals. *Soil and Tillage Research* 155:124–132.
- Karabulut S., A. Karabakan, A. Denizli, Y. Yurum. 2000. Batch removal of copper(II) and zinc(II) from aqueous solutions with low-rank Turkish coals. *Separation and Purification Technology* 18: 177–184.
- Kılıç, Murat, İsmail Kırbyık, Özge Çepelioğullar and Ayşe E. Pütün. 2013. Adsorption of heavy metal ions from aqueous solutions by bio-char, by-product of pyrolysis. *Applied Surface Science* 283:856–862.
- Lagergren, S. 1898. About the theory of so-called adsorption of soluble substances. *Kungliga Svenska Vetenskapsakademiens* 24:1–39.
- Lindsay, Willard L. 1979. *Chemical Equilibria in Soils*. John Wiley & Sons, New York.
- Suzuki, M.. 1997. Role of adsorption in water environment processes. *Water Science and Technology* 35: pp. 1–11
- Mackie, Allison L. and Margaret E. Walsh. 2012. Bench-scale study of active mine water treatment using cement kiln dust (CKD) as a neutralization agent. *Water Research* 46: 327–334.
- Mahmoued, E. K. 2010. Cement kiln dust and coal filters treatment of textile industrial effluents. *Desalination* 255:175–178.
- Meena, A.K., K. Kadirvelu, G.K. Mishraa, C. Rajagopal and P.N. Nagar. 2008. Adsorption of Pb(II) and Cd(II) metal ions from aqueous solutions by mustard husk, *J. Hazard Mater.* 150: 619–625.
- Nader, M. 2015. Surface area: Brunauer–Emmett–Teller (BET). In: *Progress in Filtration and Separation* (S. Tarleton, ed.). Academic Press, London, UK, pp. 585–608.
- Ochie, V. A., K. Trilestari, J. Sunarso, N. Indraswati and S. Ismadji. 2008. Review recent progress on biosorption of heavy metals from liquids using low cost biosorbents: Characterization, biosorption parameters and mechanism studies. *Clean* 36: 937–962.
- Park, M. and S. Komarneni. 1998. Rapid synthesis of AlPO₄-11 and cloverite by microwave hydrothermal processing. *Microporous and Mesoporous Materials* 20: 39–44.
- Paulino, A.T., F.A.S. Minasse, M.R. Guilherme, A.V. Reis, E.C. Muniz, J. Nozaki. 2006. Novel adsorbent based on silkworm chrysalides for removal of heavy metals from wastewaters. *J. Colloid Interface Sci.* 301: 479–487.
- Pigaga, A., R. Juskenas, D. Virbalyte, M.G. Klimantaviciute and V. Pakstas. 2005. The use of cement kiln dust for the removal of heavy metal ions from aqueous solutions. *Trans. Inst.Met. Finish.* 83: 210–214.
- Rahman, M. K., S. Rehman and O. S. B. Al-Amoudi. 2011. Literature review on cement kiln dust usage in soil and waste stabilization and experimental investigation *IJRRAS* 7: 77–87.
- Salem, A. and E. Velayi. 2012. Application of hydroxyapatite and cement kiln dust mixture in adsorption of lead ions from aqueous solution. *Journal of Industrial and Engineering Chemistry* 18: 1216–1222.
- Saleh, M. E., A. A. El-Refaey and A. H. Mahmoud. 2015. Effectiveness of sunflower seed husk biochar for removing copper ions from wastewater: a comparative study. *Soil & Water Research* 11: 53–63.
- Saraya, M. E. I. and M. E. Aboul-Fetouh. 2012. Utilization from cement kiln dust in removal of acid dyes. *American Journal of Environmental Sciences* 8: 16–24.
- Sari, A., M. Tuzen, Ö.D. Uluözlü and M. Soylak. 2007. Biosorption of Pb(II) and Ni(II) from aqueous solution by lichen (*Cladonia furcata*) biomass, *Biochem. Eng. J.* 37:151–158.
- Shareef, K. M. 2009. Sorbents for contaminant uptake from aqueous solution. Part I: heavy metals. *World J Agric Sci* 5:819–831.
- Sobecka, E. 2001. Changes in the iron level in the organs and tissues of wels catfish, *silurus glanis* L. caused by nickel *Acta Ichthyol. Piscat.* 31: 127–143.
- Sposito, Garrison. 1989. *The chemistry of Soils*. Oxford University press, Inc, New York.

- Suzuki, Yoshihiro, Takuji Kametani and Toshiroh Maruyama. 2005. Removal of heavy metals from aqueous solution by nonliving Ulva seaweed as biosorbent. *Water Research* 39: 1803–1808.
- Uchimiyu, M., I. M. Lima, K. T. Klasson, S. Chang, L. H. Wartelle and J. E. Rodgers. 2010. Immobilization of heavy metal ions (CuII, CdII, NiII, PbII) by broiler litter-derived biochars in water and soil. *Journal of Agricultural and Food Chemistry* 58: 5538–5544.
- Ucun, H., Y.K. Bayhan and Y. Kaya. 2008. Kinetic and thermodynamic studies of the biosorption of Cr(VI) by *Pinus sylvestris* Linn, *J. Hazard. Mater.* 153: 52–59.
- WHO. 2004. Copper in Drinking-water. World Health Organization, Geneva, Switzerland. http://www.who.int/water_sanitation_health/dwq/chemicals/copper.pdf (accessed 29 December 2016).
- Yahya, A. M., Z. Al-Qodah and C.W. Z. Ngah. 2015. Agricultural bio-waste materials as potential sustainable precursors used for activated carbon production: A review. *Renewable and Sustainable Energy Reviews* 46: 218–235.
- Zaki, Nagwan G., I.A. Khattab and N.M. Abd El-Monem. 2007. Removal of some heavy metals by CKD leachate. *Journal of Hazardous Materials* 147: 21–27.

الملخص العربي

دراسة إزالة أيونات النحاس من المحاليل المائية بواسطة التراب الإسمنتي كناتج ثانوي من صناعة الاسمنت

أحمد عبد الخالق الرفاعي

وجد تطابق واضح وبشكل جيد لنموذج الدرجة الثانية Pseudo-second-order. وأيضاً تم دراسة وحساب الثوابت الديناميكا الحرارية للتنبؤ بطبيعة الامتصاص من تغير في الطاقة الحرة (ΔG°)، المحتوى الحراري (ΔH°) والعشوائية (ΔS°). وأظهرت القيم المتحصل عليها في ظل ظروف التجربة أن حدوث هذه العملية كانت تلقائية، والتفاعل طارد للحرارة والقابلية المرتفعة لازالة ايونات النحاس من المحاليل بواسطة التراب الاسمنتي وايضا تم تقدير الذائبية والاتزان لمركبات النحاس المتوقع تكونها خلال وجود ايونات النحاس في نظام واحد مع التراب الاسمنتي واقترح أن ترسيب مركب كربونات النحاس قد يكون هو المسيطر تحت ظروف التجربة وأيد ذلك نتائج التحليل الطيفي. وبذلك أوضحت النتائج أن التراب الاسمنتي كناتج ثانوي من صناعة الاسمنت ومنخفض التكاليف يمكن أن يستخدم بكفاءة وفعالية في إزالة النحاس من المحاليل المائية.

قامت الدراسة بالتحقق من أداء التراب الإسمنتي (CKD)، كناتج ثانوي من عملية تصنيع الاسمنت، في إزالة ايونات النحاس من المحاليل المائية. وتم دراسة خواص التراب الاسمنتي بواسطة التحليل الطيفي بالأشعة تحت الحمراء (FTIR) و تحت الميكروسكوب الالكتروني وكذلك السطح النوعي لتوضيح الاختلافات في الخصائص الفيزيائية والكيميائية. أجريت تجارب ادمصاص على درجات حرارة مختلفة هي ٢٠ و ٢٥ و ٣٠°م وعلى فترات زمنية امتدت الى ٩٦ ساعة لدراسة كفاءة التراب الاسمنتي في إزالة النحاس. اظهرت النتائج الكفاءة العالية للتراب الاسمنتي في إزالة النحاس مع عدم التأثير بالتغير في درجات الحرارة. تم تأكيد النتائج بدراسة الاختلافات في التحليل الطيفي بالأشعة تحت الحمراء والدراسة تحت الميكروسكوب الالكتروني قبل وبعد تجارب الادمصااص. كما تم دراسة حركية الادمصااص من خلال النماذج المختلفة للحركية وهي نموذج الحركية الاسية fractional power، ونموذج Elovich ونموذج الدرجة الاولى والثانية.